




Article

Modeling COVID-19 Transmission in Closed Indoor Settings: An Agent-Based Approach with Comprehensive Sensitivity Analysis

Amir Hossein Ebrahimi¹, Ali Asghar Alesheikh^{1,*} , Navid Hooshangi², Mohammad Sharif^{3,*} 
and Abolfazl Mollalo⁴ 

¹ Department of Geospatial Information Systems, Faculty of Geodesy and Geomatics Engineering, K.N. Toosi University of Technology, Tehran 19967-15433, Iran; amirh.ebrahimi@email.kntu.ac.ir

² Department of Surveying Engineering, College of Earth Sciences Engineering, Arak University of Technology, Arak 38181-46763, Iran; hooshangi@arakut.ac.ir

³ Institute of Mobility and Urban Planning, University of Duisburg-Essen, 45127 Essen, Germany

⁴ Biomedical Informatics Center, Department of Public Health Sciences, Medical University of South Carolina, Charleston, SC 29425, USA; mollalo@musc.edu

* Correspondence: alesheikh@kntu.ac.ir (A.A.A.); mohammad.sharif@uni-due.de (M.S.)

Abstract: Computational simulation models have been widely used to study the dynamics of COVID-19. Among those, bottom-up approaches such as agent-based models (ABMs) can account for population heterogeneity. While many studies have addressed COVID-19 spread at various scales, insufficient studies have investigated the spread of COVID-19 within closed indoor settings. This study aims to develop an ABM to simulate the spread of COVID-19 in a closed indoor setting using three transmission sub-models. Moreover, a comprehensive sensitivity analysis encompassing 4374 scenarios is performed. The model is calibrated using data from Calabria, Italy. The results indicated a decent consistency between the observed and predicted number of infected people (MAPE = 27.94%, RMSE = 0.87 and $\chi^2(1, N = 34) = (44.11, p = 0.11)$). Notably, the transmission distance was identified as the most influential parameter in this model. In nearly all scenarios, this parameter had a significant impact on the outbreak dynamics (total cases and epidemic peak). Also, the calibration process showed that the movement of agents and the number of initial asymptomatic agents are vital model parameters to simulate COVID-19 spread accurately. The developed model may provide useful insights to investigate different scenarios and dynamics of other similar infectious diseases in closed indoor settings.

Keywords: agent-based modeling; COVID-19 transmission; sensitivity analysis; epidemiology



Citation: Ebrahimi, A.H.; Alesheikh, A.A.; Hooshangi, N.; Sharif, M.; Mollalo, A. Modeling COVID-19 Transmission in Closed Indoor Settings: An Agent-Based Approach with Comprehensive Sensitivity Analysis. *Information* **2024**, *15*, 362. <https://doi.org/10.3390/info15060362>

Academic Editors: Mario Ciampi and Mario Sicuranza

Received: 4 May 2024

Revised: 13 June 2024

Accepted: 16 June 2024

Published: 19 June 2024



Copyright: © 2024 by the authors. Licensee MDPI, Basel, Switzerland. This article is an open access article distributed under the terms and conditions of the Creative Commons Attribution (CC BY) license (<https://creativecommons.org/licenses/by/4.0/>).

1. Introduction

COVID-19, caused by SARS-CoV-2, is a highly contagious disease that spreads through various transmission pathways such as physical contact, inhalation of small particles spread by coughing or sneezing, and even indirectly through contaminated surfaces [1,2]. A high probability of infection is present inside closed indoor settings (e.g., schools, factories, or offices) due to a higher likelihood of close contact [3]. It is expected that almost 90% of transmissions occur within indoor settings [4]. Moreover, the infection risk in indoor settings is around 18.7 times higher compared to outdoor environments [5]. Although many studies have modeled COVID-19 transmission at the city and country scales, limited research has investigated the spread of COVID-19 within a closed indoor setting.

Compartmental mathematical models have a long-standing history of application in various epidemiological studies to predict and control epidemics [6]. These models are primarily based on ordinary differential equations (ODEs); however, more complex variations such as fractional or stochastic differential equations have also been developed [7]. Since the onset of the COVID-19 pandemic, numerous studies have utilized mathematical methods to investigate the behavior of this disease [8–10]. A major drawback of these compartmental

mathematical models is population heterogeneity and the neglect of interactions among individuals [11]. Moreover, these models overlook spatial components and individuals movements, which can influence the transmission dynamics [12].

Cellular automata (CA) models can address some of these limitations by modeling the spatio-temporal dynamics of diseases and reproducing the behavior of a system using local interactions [13]. Common CA models are made up of regular grids, where each cell status changes according to transition rules [14]. Their simplicity facilitates easy implementation, making them suitable for visualizing disease transmission. However, the representation of individual movements and interactions in space is not presented [15]. These models have also been used to study the spread of COVID-19 (for example, the study by Li and Yen [16]).

Agent-based modeling (ABM) is a widely employed bottom-up approach for modeling complex systems [17]. ABMs offer the advantage of incorporating population heterogeneity wherein heterogeneous agents interact with each other and the environment, leading to an emergence of the overall behavior of the system [18]. Similar to compartment and CA models, ABMs have been extensively used to simulate the spread of diseases, including malaria [19], cutaneous leishmaniasis [20], mumps [21], avian influenza [22], AIDS [23], and COVID-19 [1,24]. Besides ABMs, networked metapopulation models can also consider population diversity and spatial aspects [25]. These methods have been applied to model the spread of COVID-19 (e.g., the study by Humphries et al. (2021) [26] and the study by Calvetti et al. (2020) [27]). Since ABMs can address the mentioned shortcomings and limitations of other methods, they can provide valuable insights for modeling biological phenomena such as the spread of COVID-19. These models (ABMs) generally entail higher computational costs compared to other modeling methods [28].

In applying ABMs in COVID-19 research within indoor settings, Cuevas presented one of the initial ABMs to simulate and evaluate transmission risk at the facility scale. The model incorporated susceptible and infected agents based on four scenarios. However, the model was based on unrealistic assumptions and did not consider recovered and vaccinated cases [29]. Rodriguez et al. addressed these gaps and introduced a new ABM that included external infection, asymptomatic individuals, and vaccinated agents. They also examined five scenarios to evaluate re-opening policies in facilities, such as disinfection protocols and mobility restrictions. They validated their model using weekly infection data from McGill's University, Canada [30]. In the US, Borjigin et al. examined policies that transit agencies implemented during the early phases of COVID-19 for urban buses based on two types of agents: passengers and virus agents. Each virus agent had mobility, a life span, and a possibility of infection in case of direct contact with the passenger agents. They concluded that the most effective prevention outcome involves the combination of mask-wearing, open window policies, and half-capacity seating policy, particularly during higher-frequency bus services [31]. In Tianjin, China, Zhang et al. simulated indoor COVID-19 transmission in a supermarket with frequent human movements. They used the social force model, a microscopic ABM approach, to simulate pedestrian movement and a simple forcing method to simulate indoor airflow in their ABM. Their model included air-based transmission and surface-based transmission. The results indicated that universal mask usage was the most potent intervention while incorporating multiple exits was the most effective among spatial interventions [5].

The ABMs developed for modeling the spread of COVID-19 in indoor environments share common elements. Almost all studies in this field have examined the impact of interventions on mitigating the risk of disease. The behavior of agents is simpler in some studies and more complex in others. For example, in the Cuevas study [29], the agents' behaviors are simpler compared to the study by Gunaratne et al. [32]. In the study by Gunaratne et al., they utilized two agent-based models: one for creating a contact network and the other an agent-based SIR model. Additionally, a relatively complex scheduling program was considered for the agents. The movement of people indoors significantly influences the spread of respiratory infectious diseases [33,34]. In research related to ABMs

for simulating agent movement, various methods have been utilized. In some models, agents' movements are considered random (e.g., studies by Rodriguez et al. [30] and Karimian et al. [35]). Other studies have utilized more complex models, such as pedestrian models. For instance, Reveil and Chein used their own movement algorithm, which includes a navigation network within the simulation environment [36]. Another element is the simulation environment. The environment in ABMs simulates the spatial layout of buildings. Studies have shown that spatial layout can have a considerable impact on the spread of contagious diseases [37,38]. In some studies, the simulation environment is simple and box-like (such as Karimian et al. [35]), while in others, it is highly detailed. For example, Reveil and Chen [36] used detailed floor plans in their study to create a simulation environment. Therefore, it can be observed in the literature that agent-based models have been implemented at different resolutions, and there is always a trade-off between the complexity of the model and its execution speed.

In this study, we developed an ABM to simulate the spread of COVID-19 in indoor environments. We calibrated the model with real data to mimic the actual behavior of COVID-19 spread. The created model integrates features from previous models to enhance its reliability. This model can be used to analyze the dynamics of the disease in indoor settings (such as schools, offices, universities, and hospitals) and to examine the behavior of the disease under different scenarios. In the presented model, we assumed that COVID-19 may be transmitted in three ways: (1) transmission through direct contact with agents, (2) external transmission outside the environment, and (3) indirect disease transmission through contaminated surfaces. While previous studies focused less on indirect disease transmission through contaminated surfaces, we developed and investigated this transmission sub-model in our study. Additionally, in most previous studies on agent-based modeling of COVID-19 spread, sensitivity analysis of the developed models was either overlooked or not conducted thoroughly. Many of these studies only examined a limited number of scenarios to assess the impact of parameters on the results, creating a research gap in the sensitivity analysis of ABMs [39]. Sensitivity analysis can help assess the robustness of ABMs and understand how model parameters influence the final results. In this study, we examined the sensitivity of our model to nine parameters, resulting in 4374 different scenarios, which distinguishes our work from similar studies. To achieve this goal, we used a lower-resolution model compared to some of the high-resolution models mentioned. We demonstrated that in ABMs, it is essential to carefully examine the model's sensitivity to its parameters. This not only increases the model's reliability but also allows for a more comprehensive examination of the dynamics of disease spread, which, in turn, reveals new insights into disease prevention strategies.

2. Materials and Methods

2.1. Study Area and Data

We retrieved publicly available epidemiological data from the Calabria region in Italy [40]. The data include the number of diagnosed COVID-19 cases and the total number of conducted tests. Figure 1 shows the geographic location of the study area. The population of Calabria is over 1.8 million [41], and it spans between 15.6° E to 17.2° E longitude and 37.9° N to 40.14° N latitude, covering an area of 15,222 km². These regional-level data from Calabria were employed for meticulous model calibration, to better represent indoor disease spread dynamics, which is elaborated on in Section 2.3. The proposed ABM was implemented in NetLogo 6.2.2 open-source modeling software.



Figure 1. Geographic location of the study area.

2.2. The Agent-Based Model

The developed model incorporates human agents who can contract COVID-19 through direct and indirect contacts, as well as external infection from sources outside the defined setting. The specifications and descriptions of the ABM are presented based on the Overview, Design concepts, Details (ODD) protocol [42–44]. ODD is a protocol used to standardize the description of ABMs. Utilizing this protocol ensures the reproducibility of an ABM and prevents arbitrary descriptions of such models (something observed in previous literature), making the models comparable.

2.2.1. Purpose and Patterns

The objective of the proposed ABM is to simulate the dynamics of COVID-19 in closed indoor settings. Given the variability of the transmission parameters of COVID-19 across various strains [45], we need to evaluate the parameters under different simulation scenarios.

2.2.2. Entities, State Variables, and Scales

The developed model includes two types of entities: dynamic human agents and static cells. The state variables of human agents are shown in Table 1. It should be noted that the cells can only have location and ‘VirusConcentration’ variables. ‘VirusConcentration’ is a real number and indicates contamination of each cell.

Table 1. The state variables of human agents.

| Variable | Variable Type (Units) | Meaning |
|------------------|-----------------------|--|
| x y | Real number (meters) | position of human agents |
| $P_{Infection}$ | Real number | The probability of infection for normal human agents (Not vaccinated and without previous infection) |
| $P_{Reinfected}$ | Real number | The probability of infection of reinfected human agents |
| $P_{Vaccinated}$ | Real number | The probability of infection of vaccinated human agents |
| secretionRate | Real number | The amount of SARS-CoV-2 secretion by the infected agent |
| $P_{Fatality}$ | Real number | The probability of death of human agents |

Table 1. Cont.

| Variable | Variable Type (Units) | Meaning |
|---------------------|-----------------------|--|
| P_{Move} | Real number | The probability of movement of human agents in the environment |
| $P_{SmallMove}$ | Real number | The probability of small movement of human agents in the environment |
| $\tau_{Incubation}$ | Integer; days | Incubation time |
| $\tau_{Recovery}$ | Integer; days | Recovery time |
| State | Integer | The state of human agents (susceptible, exposed, infected, recovered, deceased, quarantined) |
| Vaccinated | Boolean | Vaccinated and unvaccinated flag |
| Asymptomatic | Boolean | Symptomatic and asymptomatic flag |
| Reinfected | Boolean | Reinfection flag |

In the present model, each time step corresponds to a single day, and the total simulation duration is one year. Human agents can be placed anywhere in this space. The simulation environment is nontoroidal. The dimensions of each cell are 1×1 meters, and the spatial extent of the model in the basic scenario is 36×36 meters. The dimensions of the environment are determined according to the study of Rodriguez et al. [30] (simulation environment: 1300 m^2 , time period: one year starting at 24 February 2020).

2.2.3. Process Overview and Scheduling

In all steps of the simulation, the sequence of agent-driven processes occurs randomly. Figure 2 outlines the procedures of the model through a flowchart diagram. At the beginning of the simulation, human agents and cells are initialized. Then, the model examines direct contacts between the agents with the potential for infection transmission. Agents can move in each time step, and after the movement procedure, surface contamination occurs when the infected agents come into contact with cells. SARS-CoV-2 has a pre-defined half-life on the cells, and its concentration on cells decreases with each time step [2]. If human agents are placed on contaminated cells, they could become infected. Lastly, our model incorporates an external infection procedure, capturing the potential for agents to contract the infection beyond the immediate simulated environment.

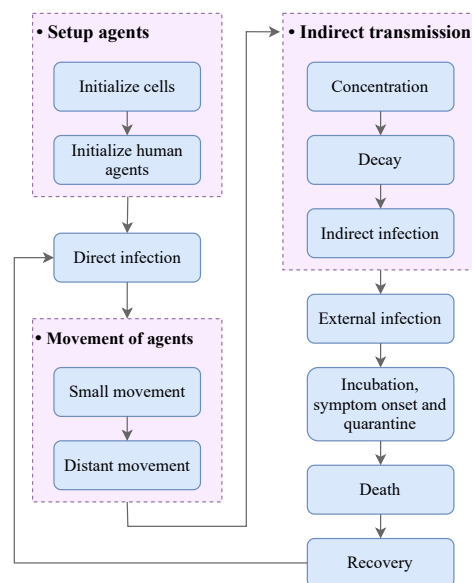


Figure 2. Procedures of the proposed model.

The clinical state of the agent is updated based on the states of the SEIRQD (Susceptible-Exposed-Infectious-Recovered-Quarantined-Deceased) model. This model includes *susceptible*, *exposed*, *infected*, *recovered*, *quarantined*, and *dead* states [46]. These state transitions are graphically depicted in Figure 3.

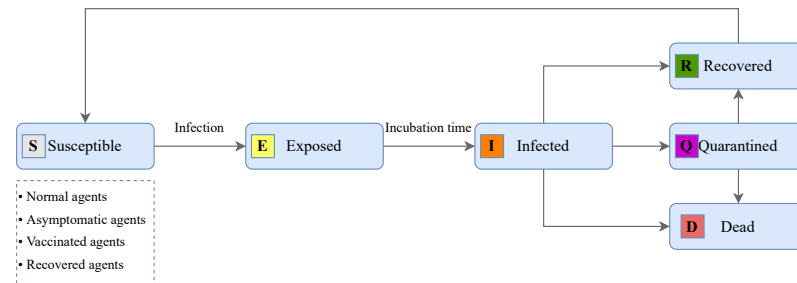


Figure 3. State of human agents in the SEIRQD model.

2.2.4. Design Concepts

Sensing

In ABMs, “sensing” refers to the ability of agents to perceive and gather information from their environment or from other agents within the system. Sensing mechanisms enable agents to interact with their surroundings, make decisions, and adapt their behaviors based on the information they receive. In our model, susceptible human agents can sense infected agents within a specific distance (transmission distance) that can be infected. Moreover, these agents can sense the cellular agents below them, leading to indirect disease transmission through contaminated surfaces. In other words, agents interact with other agents when they are within the transmission distance and, also, with their immediate environment. Cellular agents can sense infected human agents placed on them, contributing to the contamination of the environmental surface.

Interaction

In the proposed model, there are two types of interactions between agents. In the first type, infected agents can infect susceptible agents through direct physical contact. In the second type, infected agents can cause environmental contamination, and susceptible agents can become infected through cells.

Stochasticity

Stochasticity can introduce heterogeneity among agents [47]. In our model, the initialization of some state variables of agents (such as $P_{\text{Infection}}$ and $\tau_{\text{Incubation}}$) are stochastic. Moreover, the state change of agents is based on the probabilities of transition rules, and their movement is stochastic.

Observation

During the simulation, the agents and environment of the model are dynamically displayed in the user interface. The color of each agent shows its clinical state, and the color of the cells shows the concentration of SARS-CoV-2. We have displayed the statistics (for example, the number of cumulative infected agents) in charts in the user interface (see Appendix A—Figure A1).

2.2.5. Initialization

At the beginning of the simulation, state variables of agents were initialized. We considered 200 agents as the initial population of the base scenario. Table 2 presents the state variables of human agents along with the range of possible values in the base scenario. To calculate the parameters of disease transmission probabilities ($P_{\text{Infection}}$, $P_{\text{Reinfected}}$, and $P_{\text{Vaccinated}}$), we utilized the secondary attack rate calculated in other studies. It should be noted that this value is dependent on the population under study and the disease variant,

with different values being suggested in previous studies. Since our calibration data pertain to the onset of the epidemic, these values were extracted from relevant studies. The only state variable for cells is the concentration of SARS-CoV-2, with an initial value of 0.

Table 2. The initial values of state variables for human agents in the baseline scenario.

| Variable | Value | Reference/Source |
|------------------------------|-------------------------------|------------------|
| x | $[0, \textit{SettingWidth}]$ | - |
| y | $[0, \textit{SettingHeight}]$ | - |
| $P_{\textit{Infection}}$ | $[0.02, 0.03]$ | [30,48,49] |
| $P_{\textit{Reinfected}}$ | $[0.006, 0.0065]$ | [30,50] |
| $P_{\textit{Vaccinated}}$ | $[0.0045, 0.005]$ | [30,51] |
| $\textit{secretionRate}$ | 0.008 | [2] |
| $P_{\textit{Fatality}}$ | $[0.007, 0.07]$ | [30] |
| $P_{\textit{Move}}$ | $[0.3, 0.5]$ | [30] |
| $P_{\textit{SmallMove}}$ | $[0.7, 0.9]$ | [30] |
| $\tau_{\textit{Incubation}}$ | $[5, 6]$ | [52] |
| $\tau_{\textit{Recovery}}$ | 14 | [52] |
| State | <i>Susceptible</i> | - |

2.2.6. Input Data

The proposed model does not use input data to represent variations in the environment and agents. However, we have used actual data to calibrate our model as described in Section 2.3.

2.2.7. Sub-Models

We have developed several sub-models to simulate the dynamics of disease spread, with each sub-model performing a specific task. The following sub-models follow the flowchart in Figure 2.

Model Initialization

This sub-model initializes agents and the simulation environment. The parameters of the model that are initialized in this step are presented in Table 3, along with their corresponding values in the base scenario. The movement parameters (i.e., ‘*maxMovementsPerDay*’ and ‘*maxRadiusLocalMovement*’) have been adapted from the study of Rodriguez et al. within the base scenario [30]. The ‘*externalInfectionParameter*’ indicates the probability of external infection, and ‘*indirectTransmissionParameter*’ represents the probability of indirect infection. ‘*maxMovementsPerDay*’ and ‘*numberOfAsymptomaticAgents*’ are considered for model calibration as described in Section 2.3.

Table 3. The initialization parameters of the model.

| Parameter | Value |
|-------------------------------|-------|
| populationSize | 200 |
| facilityWidth | 36 |
| facilityHeight | 36 |
| simulationDays | 365 |
| maxMovementsPerDay | 350 |
| maxRadiusLocalMovement | 5 |
| distanceOfContagion | 1.5 |
| initialNumberOfInfectedAgents | 0 |
| numberOfVaccinatedAgents | 0 |
| numberOfAsymptomaticAgents | 100 |
| externalInfectionParameter | 0.015 |
| indirectTransmissionDistance | 2 |

Table 3. Cont.

| Parameter | Value |
|-------------------------------|-------|
| decayRate | 0.25 |
| secretionRate | 0.008 |
| indirectTransmissionParameter | 0.015 |

Direct Transmission Process

This sub-model simulates disease transmission via direct contact. When susceptible agents are within a specific distance (*'distanceOfContagion'*) from infected agents, they could become infected with a certain probability ($P_{\text{Infection}}$). The probability of infection is also proportional to the agents' states. For agents who have previously recovered, the probability of infection is lower due to increased immunity ($P_{\text{Reinfected}}$). Vaccinated agents have the least infection probability ($P_{\text{Vaccinated}}$).

Movement of Agents

This sub-model simulates the movement of agents within a setting. The movement of agents is the primary reason for their interaction with each other and consequently for disease transmission. For this reason, one of the earliest and most effective non-pharmaceutical interventions for disease prevention is social distancing. Various studies have employed different models to simulate agent movement. In studies conducted on smaller scales (such as cities and countries), agent movement is often not explicitly modeled, and instead, disease transmission networks are used (as in the study by Kerr et al. [53]). In network-based models (such as metapopulation models), it is the movement and migration of the population that ultimately leads to the spread of the disease [25,54,55]. Given the large number of agents in these studies, a precise definition of agent movement at a finer temporal resolution may not be feasible. However, in indoor studies, agent movement is usually modeled. This practice leads to simulations that closely resemble reality. In indoor environments (such as schools or offices), individuals typically engage in various movements throughout the day (such as going to the restroom or picking up a tool). To model the movement of individuals, similar to the Rodriguez et al. model, we considered two types of movement for agents: small and large movements [30]. In each time step (one day), agents must perform a certain number of movements determined by a parameter, *'maxMovementsPerDay'*. In this sub-model, each agent first decides, based on a probability P_{Move} , whether to move or remain stationary. If the decision is to move, it then decides, with probability $P_{\text{SmallMove}}$, whether to make a small or large movement. The probability of making a small movement is higher than that of making a large movement. In a small movement, the agent moves in a random direction within a radius *'maxRadiusLocalMovement'*. In a large movement, the agent's position is randomly determined within the simulation space. This process is repeated for all agents multiple times until, ultimately, in each time step, simulation, *'maxMovementsPerDay'* movements are performed.

Indirect Transmission Process

This sub-model accounts for disease transmission through contaminated surfaces. The infected agents contaminate their environment by releasing droplets containing SARS-CoV-2 at a rate of *'secretionRate'* within a radius of *'indirectTransmissionDistance'*. The *'decayRate'* is considered based on the half-life of SARS-CoV-2 on surfaces. The agents could be infected based on indirect transmission probability, determined by the probability of *'indirectTransmissionParameter'* multiplied by *'virusconcentration'*.

External Infection Process

Assuming external infection outside the immediate setting, *'externalInfectionParameter'* is the probability of transmission outside the setting. At each step, agents could be infected

through external sources which simulate the contagion dynamics of locality (city, state, country) [30].

Incubation and Quarantine Process

Exposed agents are initially asymptomatic and may develop symptoms after the incubation period. Asymptomatic agents remain in the setting when infected, while symptomatic agents are quarantined after the incubation period until they recover and cannot transmit the disease during the quarantine period.

Agents' Mortality Process

This sub-model simulates the mortality process. Since asymptomatic agents have mild symptoms, only quarantined agents may die. The probability of death for vaccinated agents is decreased by 90% [56].

Recovery Process

As COVID-19 patients usually recover within a few days, in this sub-model, the infected agents recover after the recovery period. The recovered agents may be reinfected, but their probability of infection is lower due to their enhanced immunity [57].

2.3. Model Calibration

We calibrated our model similar to the study of Bouchnita and Jebrane [2]. They calibrated their multi-scale model with a population of 250 agents using data from the Calabria region, Italy. Given the limited number of calibration parameters in our model, we calibrated the model manually.

The calibration data were for the early days of the epidemic and were collected for 35 days starting from 24 February 2020. Our preliminary descriptive statistics showed that a total of 614 infected cases have been recorded (max = 101, min = 0, mean = 18 per day, standard deviation = 23). In addition to the daily infections, this dataset included daily total tests. We used the infected population rate to align the data population with our simulation population.

Figure 4 shows the daily counts of infected cases and the corresponding histogram for calibration and real data. We considered the average results of 1000 simulation runs in calibration. Two parameters were estimated in the calibration process: *'maxMovementsPerDay'* and *'numberOfAsymptomaticAgents'*. The corresponding values are mentioned in Table 3.

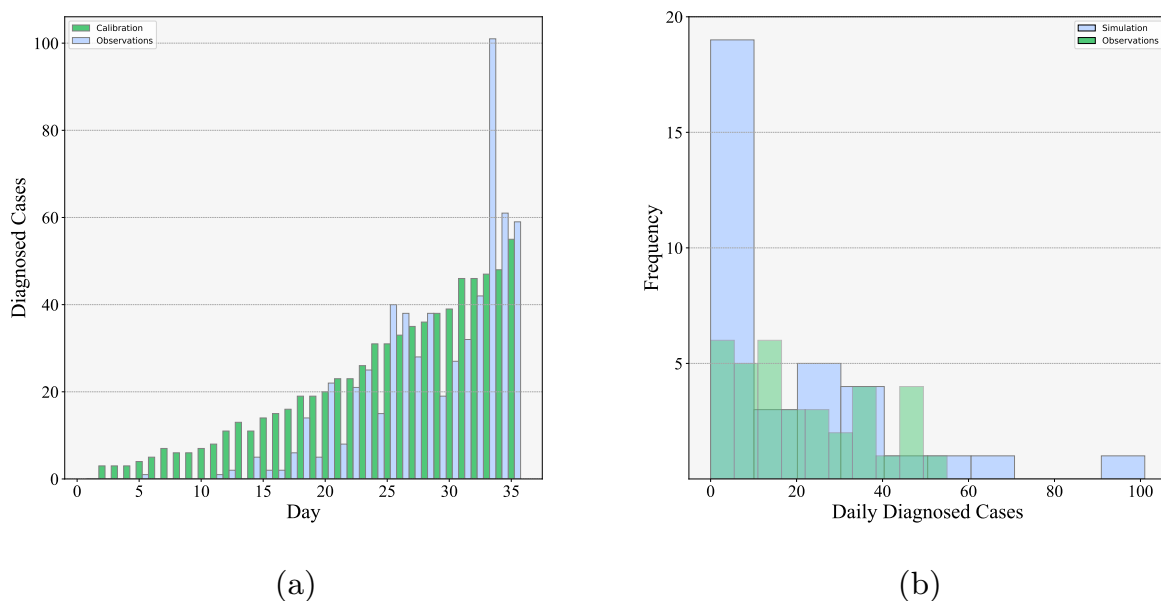


Figure 4. Infected cases: (a) Calabria daily data and (b) data distribution.

To compare the simulation results with the actual data, three evaluation metrics, including RMSE (Root-Mean-Square Error), normalized RMSE (NRMSE), and MAPE (Mean Absolute Percentage Error) were used. Also, we used the Chi-square goodness-of-fit test to assess how close the values predicted by the model are to the actual data [24].

2.4. Sensitivity Analysis

The sensitivity analysis methodology employed in our proposed model is similar to the protocol provided by Borgonovo et al. [39]. This protocol is more comprehensive than the usual scenario-based methods used in many studies that examine a limited number of scenarios. In our sensitivity analysis, we explored a substantial number of scenarios and visualized the results using simple ICE (Individual Conditional Expectation) diagrams. The sensitivity analysis parameters, their values, and base scenario values are presented in Table 4.

Table 4. The sensitivity analysis parameters of the model.

| Parameter | Values | Base Scenario Value |
|-------------------------------|------------------------|---------------------|
| distanceOfContagion | 1,5,2 | 1.5 |
| recoveryTime | 10, 14, 18 | 14 |
| facilityWidth | 30, 36, 40 | 36 |
| facilityHeight | | |
| maxMovementsPerDay | 250, 305, 350 | 350 |
| incubationTimeRange | [3, 4], [5, 6], [7, 8] | [5, 6] |
| initialNumberOfInfectedAgents | 0, 5, 10 | 0 |
| numberOfVaccinatedAgents | 0, 20, 40 | 0 |
| numberOfAsymptomaticAgents | 50, 100, 150 | 100 |

According to Table 4, all combinations of sensitivity analysis parameters of the model produced 4374 different scenarios. Comparing these scenarios with each other allows for checking the effect of the parameters in the model. It should be noted that due to the stochastic nature of the model, scenarios need to be repeated multiple times to overcome randomness, and conclusions are based on the average results. To address this, we repeated each scenario 20 times and based our analysis on the average of these results. Furthermore, since only the effect of the parameter under investigation was to be examined, corresponding scenarios were executed using the same random seed. Finally, the total number of runs equals $4374 \times 20 = 87480$. The execution time of each scenario can be different according to its parameters (such as ‘maxMovementsPerDay’ and ‘facilityWidth’). However, the execution time of all scenarios, along with their repetitions, was about 24 h on a machine with an Intel® Core™i5-8250U processor and 12 GB of RAM.

3. Results

3.1. Calibration

The Kolmogorov–Smirnov test showed that the data do not follow a normal distribution, $D(35) = 0.63, p = 0.00$. According to the calibration analysis, the values for the evaluation of the model were RMSE = 0.87 infected people, NRMSE = 6%, and MAPE = 27.94% which indicates a decent consistency between the actual data and results [47]. Also, the Chi-square test revealed that the simulation results and actual data are not significantly different [$\chi^2(1, N = 34) = (44.11, p = 0.11)$].

In Figure 5, the real data from Calabria, Italy, are shown alongside the results obtained from averaging 1000 simulation repetitions. During the calibration process, it was found that the ‘maxMovementsPerDay’ parameter is the most crucial parameter aligning the model with reality. The curvature of the simulation results in this figure is heavily influenced by this parameter, and without considering this parameter, the cumulative growth rate of infected cases is almost linear. This shows the importance of the ‘maxMovementsPerDay’ parameter and the movements of agents in the spread of COVID-19.

We have plotted the maximum, minimum, and interquartiles of the simulation to show that the model is very sensitive to randomness. At the beginning of the simulation, the interquartiles are close to the average, but in the next time steps, their distance from the average significantly increases. The minimum (which is zero in all these 35 days) and maximum simulation curves are very different from the average curve. The stochasticity of the model justifies this significant differences between the simulation runs. In this figure, we can visually observe that the model demonstrates a better alignment with the actual data in the final days (day 20 onwards). The data from Calabria, Italy, include COVID-19 tests conducted as well. Testing conducted in the early days of the outbreak is comparatively lower than in later days, which is likely why the model fits better in the later days. It is crucial to acknowledge, however, that the model's design and overall accuracy also significantly impact its performance.

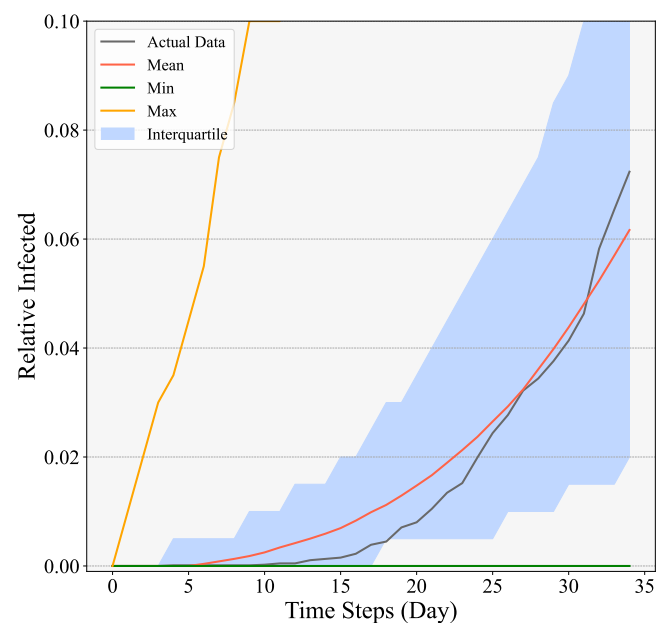
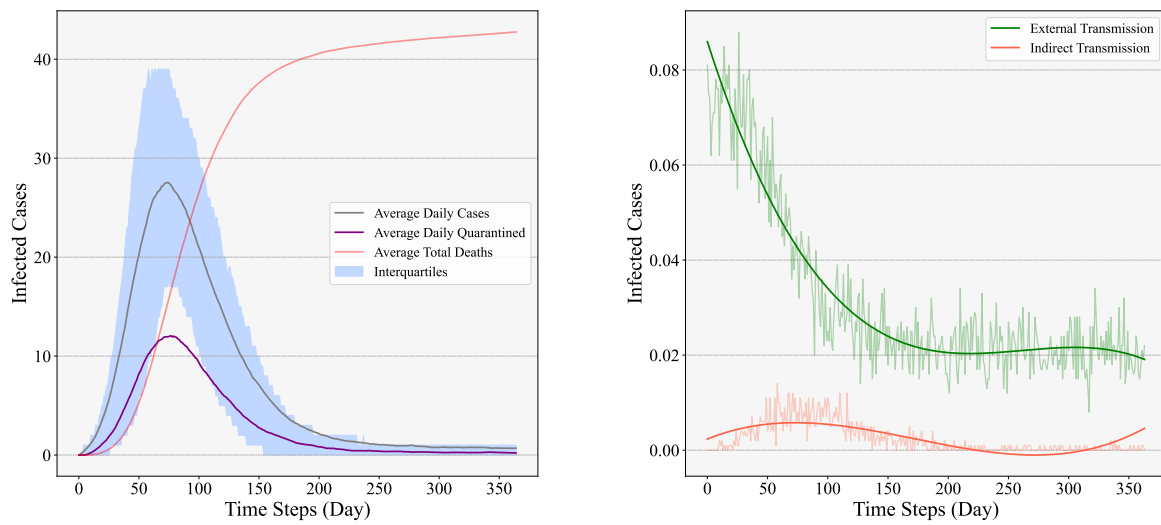


Figure 5. Comparison chart of calibration results and data from Calabria, Italy.

3.2. Base Scenario Dynamics

In Figure 6a, depicting the dynamics of mortality, infection cases, and the number of individuals in quarantine during the spread of COVID-19 (results obtained from averaging 1000 model runs), at the onset of the outbreak, due to the lack of immunity among individuals, the disease spreads rapidly. The peak of the outbreak occurs on average on day 75, and 27.25 new cases are infected with COVID-19 on this day. The basic reproduction number calculated for the simulation results was 2.414, while for the real data, it was 2.934. We used the Initial Exponential Growth Method to calculate these values [58,59]. These numbers are consistent with previous studies that suggest values for Italy in the range of 2.5 to 3.0 [60]. In calculating this value, quarantined agents that did not play a role in disease transmission were not considered. The peak of quarantined and dead agents is also in this time step. After the peak, the number of daily cases, quarantined agents and deaths decrease due to increased immunity of the agents.

The results show that most agents were infected through direct contact. 94.28% of cases were infected through direct transmission, while 5.30% of cases were through external infection, and only 0.42% were through indirect infection. Figure 6b shows that the number of infected cases through external infection is decreasing during the simulation, and the peak of the number of infected cases through indirect infection occurs at the same time as the peak of outbreak.



(a) (b)

Figure 6. Base scenario simulation results: (a) dynamics of simulation and (b) external and indirect transmission dynamics.

3.3. Sensitivity Analysis

In the sensitivity analysis, we compared the results of each scenario with other scenarios from three points of view: (1) the total number of infected cases, (2) the number of infected cases at the outbreak peak, and (3) the time step of the outbreak peak. Figure 7 illustrates the changes in the total number of infected cases with respect to each parameter of the sensitivity analysis. Each blue or red line corresponds to two scenarios that differ only in the parameters of the diagram. The horizontal axis corresponds to the values considered for the sensitivity analysis parameters, and the vertical axis shows the ratio of the total number of infected agents in each scenario to the initial population. This ratio is shown with black solid circles created as vertical lines in diagrams. The larger black solid circles show the average of this ratio for each parameter value. Similarly, the diagrams of the number of infected cases at peak and the time of the outbreak peak are produced (see Appendix B—Figure A2 and Appendix B.2—Figure A3).

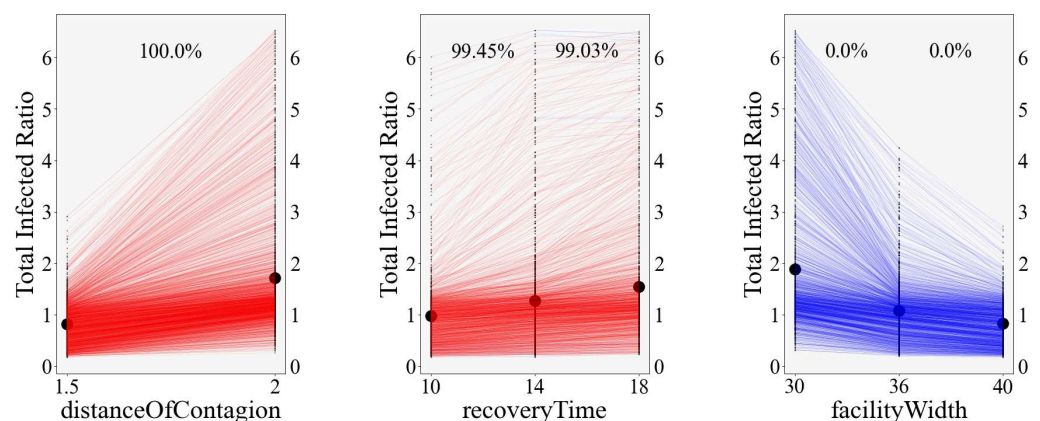


Figure 7. Cont.

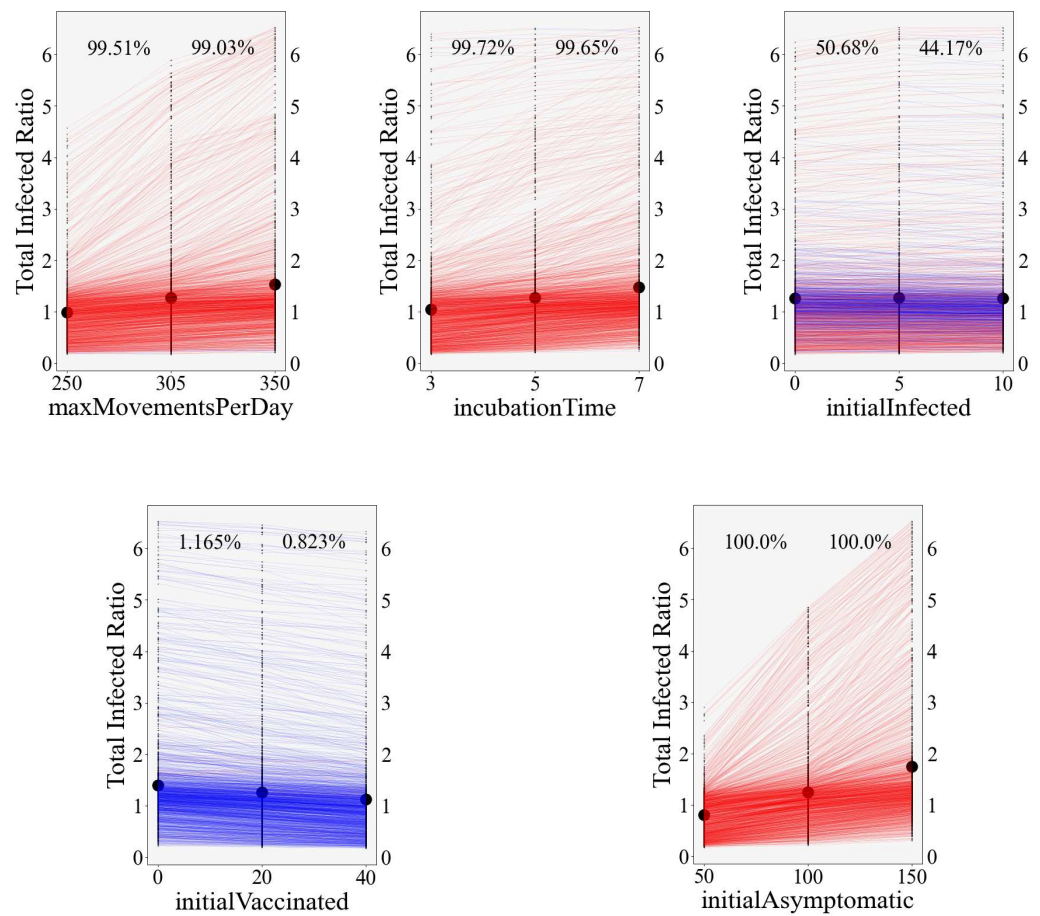


Figure 7. Comprehensive sensitivity analysis results: (The red lines from left to right show an increase in the total number of infected agents, and the blue lines show a decrease in infected agents. The numbers above each diagram indicate the percentage of red lines for each pair of parameters).

To quantitatively examine the effect of each parameter, we have used the average differences between the corresponding scenarios. The greater the difference, the greater the effect of that parameter in the model. Table 5 presents the sensitivity analysis statistics.

Table 5. Results of model sensitivity analysis.

| Parameters * | Total Infected | | | | Infected at Peak | | | | Peak Time | | | |
|--------------|----------------|-------|----------|-------|------------------|-------|----------|--------|-------------|-------|----------|--------|
| | % Red Lines | | Avg Diff | | % Red Lines | | Avg Diff | | % Red Lines | | Avg Diff | |
| P_1 | 100 | | 0.89 | | 100 | | 37.38 | | 12.52 | | -23.28 | |
| P_2 | 99.45 | 99.03 | 0.29 | 0.28 | 97.18 | 96.02 | 9.95 | 8.09 | 65.70 | 66.94 | 1.69 | 1.80 |
| P_3 | 0.00 | 0.00 | -0.81 | -0.24 | 0.00 | 0.14 | -25.13 | -13.12 | 90.26 | 79.01 | 14.16 | 8.72 |
| P_4 | 99.51 | 99.03 | 0.29 | 0.26 | 98.42 | 99.24 | 9.48 | 7.89 | 32.92 | 15.43 | -1.92 | -7.11 |
| P_5 | 99.72 | 99.65 | 0.22 | 0.21 | 100 | 99.93 | 13.46 | 13.40 | 36.07 | 33.19 | -5.24 | -4.03 |
| P_6 | 50.68 | 44.17 | 0.012 | 0.00 | 76.13 | 88.34 | 1.63 | 3.27 | 0.07 | 0.27 | -46.23 | -17.83 |
| P_7 | 1.17 | 0.82 | -0.14 | -0.14 | 1.30 | 2.19 | -9.00 | -8.37 | 71.87 | 75.50 | 3.49 | 3.52 |
| P_8 | 100 | 100 | 0.44 | 0.50 | 99.93 | 100 | 21.80 | 25.86 | 48.35 | 36.21 | -4.28 | -5.18 |

* Parameters are: P_1 : Distance of Contagion, P_2 : τ_{Recovery} , P_3 : Facility Width, P_4 : Max Movements Per Day, P_5 : $\tau_{\text{Incubation}}$, P_6 : Initial Number of Infected Agents, P_7 : Number of Vaccinated Agents and P_8 : Number of Asymptomatic Agents.

3.3.1. Total Infections

The “Total Infected” column in Table 5 represents the COVID-19 infection rate. The results show that ‘DistanceOfContagion’ is the most influential parameter on total infections.

In 100% of scenarios, the increase in this parameter has increased the total number of infected people by 89% of the initial population. It can be observed from this table that increasing the dimensions of the environment (*facilityWidth*) from 30 to 36 results in a reduction in the infection rate by 0.81, reaching 38 individuals. Moreover, the results show that increasing this parameter is less effective in larger environments to control the total infections. In other words, increasing the dimensions of the environment from 36 to 40 has only reduced the infection rate by 0.24. *numberOfAsymptomaticAgents* parameter is identified as the third most influential parameter; increasing the number of asymptomatic agents from 100 to 150 leads to a 0.5 increase in the infection rate. In other words, in this scenario, the number of infected individuals increases by 100. The parameters τ_{Recovery} , *maxMovementsPerDay*, and $\tau_{\text{Incubation}}$ have had a nearly equal effect on the total infection rate. On average, they have increased the infection rate by 0.25 (equivalent to 40 individuals). *numberOfVaccinatedAgents* has reduced the total infection rate by 0.14 (equivalent to 28 individuals). *initialNumberOfInfectedAgents* has almost no effect on the total number of infected cases.

3.3.2. Number of Infected Cases at Peak

The second column of Table 5 represents the number of individuals infected at the peak of the epidemic. In the baseline scenario, during the peak time step of the epidemic, there were approximately 27 cases of infection. *DistanceOfContagion* was the most influential parameter as we mentioned in the last section. The increase in this parameter led to an increase in infected cases in the peak by an average of 37.38 people (139% of the base scenario). The results indicate that with an increase in the number of asymptomatic agents (*DistanceOfContagion*) from 100 to 150, on average, an additional 25.86 individuals became infected during the peak time step of the disease (up to about 95% of the results of the base scenario). The effect of the *facilityWidth* parameter was similar to its effect on the total number of infected cases. Moreover, the three parameters of $\tau_{\text{Incubation}}$, τ_{Recovery} and *maxMovementsPerDay* had a similar performance, but unlike the previous section, the effect of $\tau_{\text{Incubation}}$ was greater than the other two parameters in peak cases. The effect of the *numberOfVaccinatedAgents* on the number of peak cases was more than the total number of cases, and it was the same as the three mentioned parameters. This parameter reduced the number of cases in the peak by an average of nine people (33% compared to the base scenario). The *initialNumberOfInfectedAgents* had the least effect in cases of peak infection (about 7% compared to the base scenario).

3.3.3. The Peak Time Step

The third column of Table 5 depicts the time step at which the epidemic peaks, which was on day 75 in the baseline scenario. Unlike the two previous sections, the most influential parameter in determining the peak time step was the *initialNumberOfInfectedAgents*. Increasing the initial infected from 0 to 5 resulted in a reduction of 46.23 time steps in the peak time step of the disease (a 61% decrease compared to the baseline scenario). The *DistanceOfContagion* parameter also showed the same behavior (31.4% compared to the base scenario). Increasing the *facilityWidth* parameter delayed the peak time step by 14.16 days (18.88% compared to the base scenario). The impact of other parameters was less than 10% compared to the base scenario, but in general, the increase in the *numberOfVaccinatedAgents* and τ_{Recovery} parameters caused the delay of the peak day, and the *numberOfAsymptomaticAgents*, $\tau_{\text{Incubation}}$, and *maxMovementsPerDay* parameters accelerated reaching the peak.

4. Discussion

This study proposed an ABM to simulate COVID-19 spread in closed indoor settings, employing three different sub-models. Within this framework, agents could interact with each other and the environment and become infected through direct, indirect and external contacts. However, most infections were through the direct transmission sub-model. Infection rates decreased over time as people developed immunity in all three transmission

sub-models. The developed model could evaluate different scenarios, and by modifying the parameters of the model, it could investigate the dynamics of other strains of COVID-19 (or even similar infectious diseases), each with distinct characteristics. Therefore, the proposed model can be used to make appropriate decisions to control or reduce the spread of the disease.

A total of 4374 different scenarios were examined, and the results implied that the distance of contagion was the most influential parameter. This massive number of scenarios allowed for a more thorough exploration of the parameter space and its influence on the results. This compelled us to strike a trade-off between the complexity of the model and its computational cost, resulting in a lower resolution of our results. While using more complex sub-models could potentially lead to a more accurately calibrated model, the possibility of sensitivity analysis of its parameters to this extent was not feasible, distinguishing our work from other studies. While there are limited studies on closed indoor settings using ABM, the proposed model is consistent with the prevailing findings. For instance, like Bouchnita and Jebrane [2], we concluded that by reducing the mobility of the agents, the number of total infection cases decreased, and the epidemic curve became flatter.

Rodriguez et al. examined the mobility restrictions scenario in their model and concluded that this measure did not significantly reduce the risk of contagion which is similar to our results [30]. Social distancing and mask-wearing scenarios were implemented by altering the inherent parameters of the disease in the study conducted by Mahdizadeh Gharakhanlou and Hooshangi [52]. Similarly, we showed that these parameters significantly influence the dynamics of COVID-19. Zhang et al. indicated that the unreasonable spatial layout of the setting, leading to congestion of people, could significantly increase the risk of infection [5]. In the same way, we identified that the spatial layout of the setting is one of the most influential parameters affecting the infection results. Furthermore, in their model, disease transmission from surfaces occurs rarely. During the calibration process, we identified, through testing appropriate values for the calibration parameters, that for closer alignment of the model with reality, it is necessary for the probability of disease transmission through surfaces to be very low, which is consistent with their results.

We found that the primary mode of infection is through direct transmission (94.28%) inside the setting, which is consistent with previous COVID-19 studies [4]. External infection rarely occurs in the model, but the initiation of the outbreak is completely dependent on it. Indirect transmission also occurs very little due to the low probability of infection and the considered half-life. The sensitivity analysis results showed that the settings dimensions are the most influential parameters on both the total number of cases and the number of cases at the disease peak. Additionally, the initial number of agents affected by the disease is the most influential parameter on the timing of the disease peak. Our analysis showed that the intrinsic parameters of COVID-19 (such as incubation time, recovery period, and especially distance of contagion) have a great impact on the epidemic curve. These results suggest that measures related to these parameters (such as mask-wearing) can be very effective in controlling COVID-19 in indoor settings. Also, according to the analysis, we realized that the dimensions of the setting are one of the most important parameters. By increasing the dimensions of the environment, the direct contact between the agents is reduced, and as a result, the cases of infection are reduced. The results suggest that avoiding crowded closed settings can greatly reduce the possibility of disease transmission. The more open the setting, the less chance of infection. The number of asymptomatic agents is also very effective in spreading the disease. After infection, these agents remain in the model environment and are not quarantined, thus increasing the infection rate. Identification of asymptomatic agents can effectively control epidemics within closed indoor settings.

There are some limitations in this study that should be acknowledged. Firstly, in this study, we extracted the model parameters from previous studies. Although the model with the current parameters can effectively replicate real-world data, these parameters do not have consistent values across different studies and are not identical. Therefore, the values used for model parameters are always subject to uncertainty and should be investigated.

One of the objectives of the conducted sensitivity analysis was to assess how sensitive the model is to the values of these parameters, but further investigation is required. Secondly, we used a limited number of sub-models to produce COVID-19 dynamics to keep the computational cost of the model as low as possible. The conducted sensitivity analysis method is not applicable for models with high computational costs as it requires a high number of scenarios. Using more complex sub-models and providing a method to control the computational cost can help to increase the accuracy of the model. Also, we abstracted the setting in a simple environment in the model, and it could be enriched by real spatial data. Thirdly, while the conducted sensitivity analysis comprehensively describes the model's behavior, it is always possible to enrich the sensitivity analysis by adding new parameters, examining parameters on a finer scale, and even exploring sensitivity analyses of other sub-models. However, this expansion is somewhat limited by computational constraints. Finally, we used data and methods from previous studies that could have uncertainties not examined thoroughly. These uncertainties directly affect the results and should be investigated more deeply.

The models developed in future works can be enriched by more data, such as spatial data, as well as other sub-models, which can increase the computational complexity of these models. Additionally, more parameters can be examined in sensitivity analysis to determine their impact on the dynamics of the disease. Also, since running a large number of scenarios in models with a high computational cost is challenging, developing a method to reduce the number of scenarios or the necessary repetitions of each scenario can be helpful in more complex models, which can be investigated in future research. Further investigation into the spatial aspects, such as the positions of agents, the shape of the environment, the arrangement of objects like shelves and chairs, the locations and number of rooms, the positions and number of ventilation openings, and the number of floors, are all factors that, utilizing the analyses conducted in this study, can be examined in a separate spatial study.

5. Conclusions

Our study aimed to employ agent-based models for simulating COVID-19 transmission dynamics in indoor closed settings. We conducted a thorough sensitivity analysis on model parameters, offering a novel approach within the subject's literature. The adaptable nature of the model allows for its application in studying various infectious diseases by adjusting parameters. Our model's flexibility facilitates its application across diverse indoor environments through parameter modifications, including adjustments to agent population, simulation environment, and disease transmission parameters. Our findings underscore the significant impact of parameters such as the number of asymptomatic agents, simulation environment dimensions, disease recovery time, and incubation period on model dynamics. Through sensitivity analysis, the effects of other parameters can also be examined, a practice often overlooked in the existing literature. Our study highlights the necessity of assessing the sensitivity of agent-based models to parameter uncertainty, particularly in epidemiological contexts.

Author Contributions: Conceptualization, A.H.E.; Methodology, A.H.E.; Software, A.H.E.; Validation, all authors; Formal analysis, A.H.E.; Investigation, all authors; Writing—original draft, A.H.E. and N.H.; Writing—review and editing, all authors; Visualization, A.H.E. and A.M.; Supervision, A.A.A. and N.H.; Project administration, A.A.A. All authors have read and agreed to the published version of the manuscript.

Funding: This research received no external funding.

Institutional Review Board Statement: Not applicable.

Informed Consent Statement: Not applicable.

Data Availability Statement: The data underlying this article will be shared on reasonable request to the corresponding author.

Conflicts of Interest: The authors declare no conflicts of interest.

Appendix A

You can see the model user interface in Figure A1.

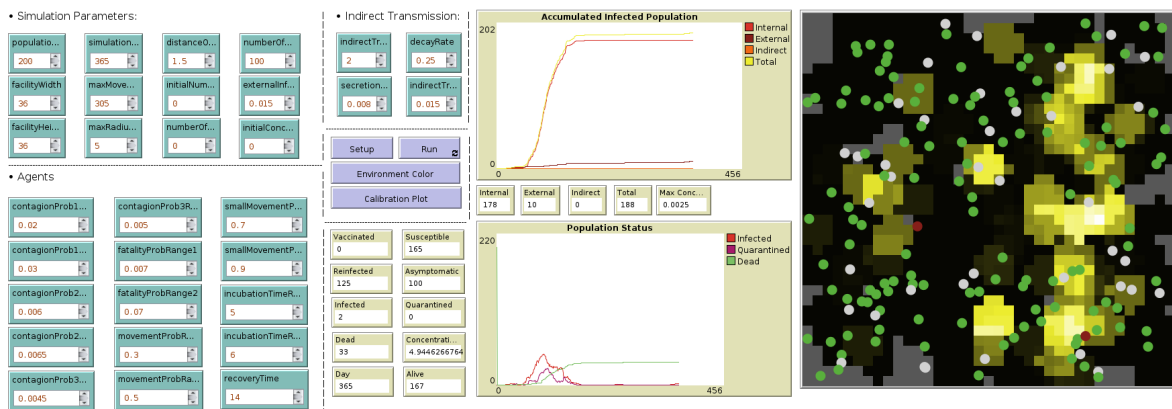


Figure A1. User interface of the proposed model. On the left are the model parameters and variables. The center of the figure displays the epidemic charts and a summary of the model outputs. The right side shows the simulation environment and agents. The color of the environment indicates the level of contamination, while the color of the agents indicates their status.

Appendix B

Appendix B.1

Sensitivity results of peak time are depicted in Figure A2.

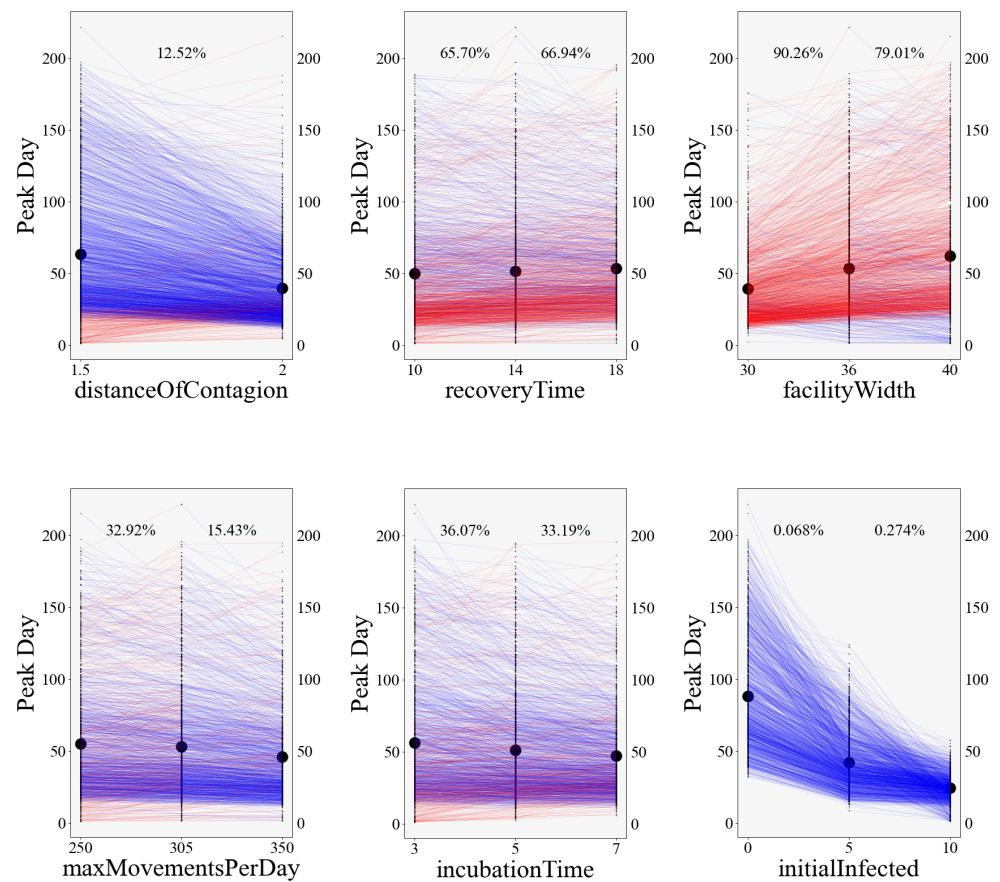


Figure A2. Cont.

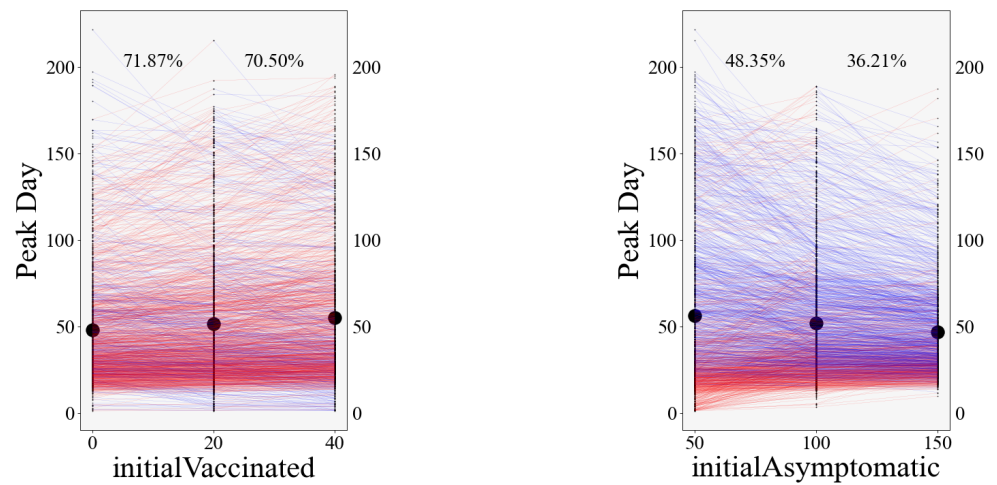


Figure A2. Sensitivity analysis results (peak time step). The red lines indicate an increase in the peak time of the disease, while the blue lines indicate a decrease.

Appendix B.2

Sensitivity results of total cases at peak are depicted in Figure A3.

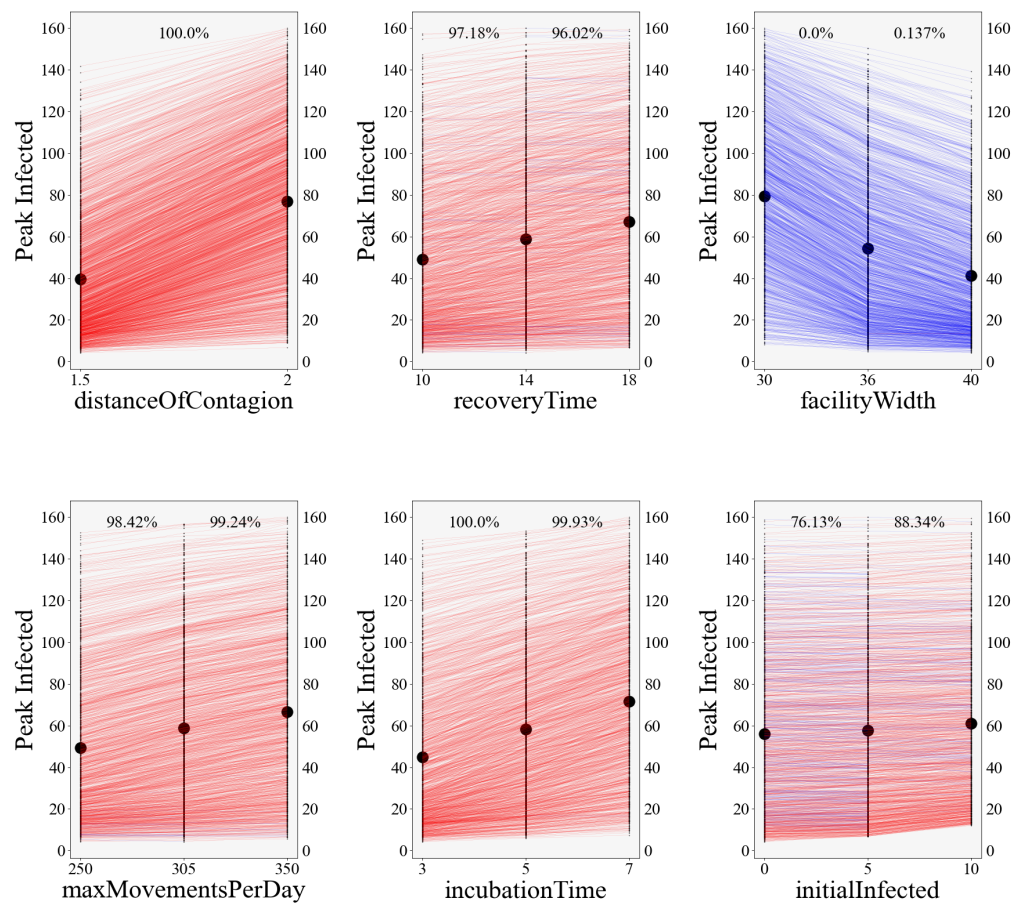


Figure A3. Cont.

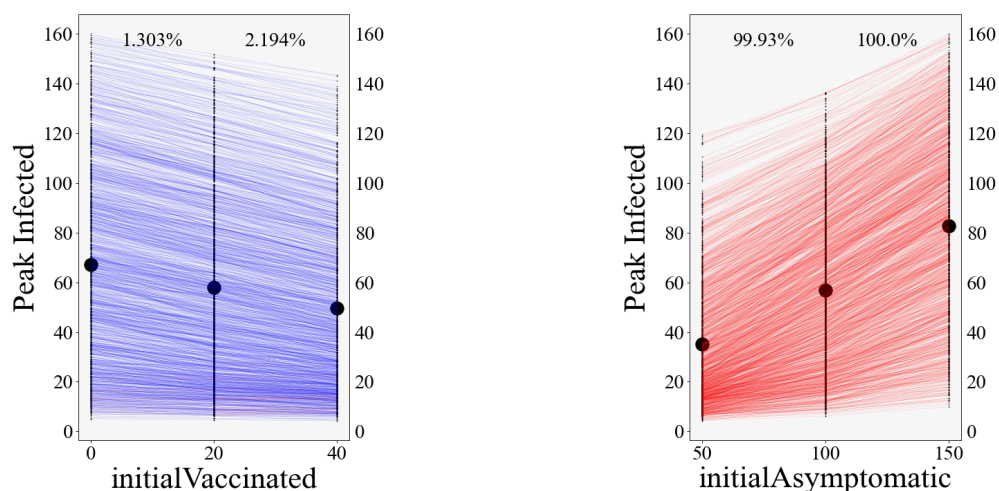


Figure A3. Sensitivity analysis results (total cases at peak). The red lines indicate an increase in the number of cases at the peak of the disease, while the blue lines indicate a decrease.

References

- Chen, K.; Li, Y.; Zhou, R.; Jiang, X. A stochastic agent-based model to evaluate COVID-19 transmission influenced by human mobility. *arXiv* **2022**. [\[CrossRef\]](#)
- Bouchnita, A.; Jebrane, A. A hybrid multi-scale model of COVID-19 transmission dynamics to assess the potential of non-pharmaceutical interventions. *Chaos Solitons Fractals* **2020**, *138*, 109941. [\[CrossRef\]](#)
- Noorimotlagh, Z.; Jaafarzadeh, N.; Martínez, S.S.; Mirzaee, S.A. A systematic review of possible airborne transmission of the COVID-19 virus (SARS-CoV-2) in the indoor air environment. *Environ. Res.* **2021**, *193*, 110612. [\[CrossRef\]](#)
- Bulfone, T.C.; Malekinejad, M.; Rutherford, G.W.; Razani, N. Outdoor Transmission of SARS-CoV-2 and Other Respiratory Viruses: A Systematic Review. *J. Infect. Dis.* **2020**, *223*, 550–561. [\[CrossRef\]](#)
- Zhang, A.; Zhen, Q.; Zheng, C.; Li, J.; Zheng, Y.; Du, Y.; Huang, Q.; Zhang, Q. Assessing the impact of architectural and behavioral interventions for controlling indoor COVID-19 infection risk: An agent-based approach. *J. Build. Eng.* **2023**, *74*, 106807. [\[CrossRef\]](#)
- Avram, F.; Adenane, R.; Ketcheson, D.I. A Review of Matrix SIR Arino Epidemic Models. *Mathematics* **2021**, *9*, 1513. [\[CrossRef\]](#)
- Lima, L.d.S. Fractional Stochastic Differential Equation Approach for Spreading of Diseases. *Entropy* **2022**, *24*, 719. [\[CrossRef\]](#)
- Adiga, A.; Dubhashi, D.; Lewis, B.; Marathe, M.; Venkatramanan, S.; Vullikanti, A. Mathematical Models for COVID-19 Pandemic: A Comparative Analysis. *J. Indian Inst. Sci.* **2020**, *100*, 793–807. [\[CrossRef\]](#)
- Vytla, V.; Ramakuri, S.K.; Peddi, A.; Kalyan Srinivas, K.; Nithish Ragav, N. Mathematical Models for Predicting COVID-19 Pandemic: A Review. *J. Phys. Conf. Ser.* **2021**, *1797*, 012009. [\[CrossRef\]](#)
- Shankar, S.; Mohakuda, S.S.; Kumar, A.; Nazneen, P.S.; Yadav, A.K.; Chatterjee, K.; Chatterjee, K. Systematic review of predictive mathematical models of COVID-19 epidemic. *Med. J. Armed Forces India* **2021**, *77*, S385–S392. [\[CrossRef\]](#)
- Zachreson, C.; Chang, S.; Harding, N.; Prokopenko, M. The effects of local homogeneity assumptions in metapopulation models of infectious disease. *R. Soc. Open Sci.* **2022**, *9*, 211919. [\[CrossRef\]](#)
- Mehdaoui, M. A review of commonly used compartmental models in epidemiology, *arXiv* **2021**. [\[CrossRef\]](#)
- Seck-Tuoh-Mora, J.C.; Hernandez-Romero, N.; Lagos-Eulogio, P.; Medina-Marin, J.; Zuñiga-Peña, N.S. A continuous-state cellular automata algorithm for global optimization. *Expert Syst. Appl.* **2021**, *177*, 114930. [\[CrossRef\]](#)
- Li, J.; Xiang, T.; He, L. Modeling epidemic spread in transportation networks: A review. *J. Traffic Transp. Eng. (Engl. Ed.)* **2021**, *8*, 139–152. [\[CrossRef\]](#)
- Perez, L.; Dragicevic, S. An agent-based approach for modeling dynamics of contagious disease spread. *Int. J. Health Geogr.* **2009**, *8*, 50. [\[CrossRef\]](#)
- Li, C.Y.; Yin, J. A pedestrian-based model for simulating COVID-19 transmission on college campus. *Transp. A Transp. Sci.* **2023**, *19*, 2005182. [\[CrossRef\]](#)
- Hooshangi, N.; Alesheikh, A.A.; Panahi, M.; Lee, S. Urban search and rescue (USAR) simulation system: Spatial strategies for agent task allocation under uncertain conditions. *Nat. Hazards Earth Syst. Sci.* **2021**, *21*, 3449–3463. [\[CrossRef\]](#)
- Wilensky, U.; Rand, W. *An Introduction to Agent-Based Modeling: Modeling Natural, Social, and Engineered Complex Systems with NetLogo*; The MIT Press: Cambridge, MA, USA, 2015.
- Layie, P.; Kamla, V.C.; Kamgang, J.C.; Wono, Y.E. Agent-based modeling of malaria control through mosquito aquatic habitats management in a traditional sub-Saharan grouping. *BMC Public Health* **2021**, *21*, 487. [\[CrossRef\]](#)
- Rajabi, M.; Pilesjö, P.; Shirzadi, M.R.; Fadaei, R.; Mansourian, A. A spatially explicit agent-based modeling approach for the spread of Cutaneous Leishmaniasis disease in central Iran, Isfahan. *Environ. Model. Softw.* **2016**, *82*, 330–346. [\[CrossRef\]](#)

21. Simões, J., An Agent-Based/Network Approach to Spatial Epidemics; In *Agent-Based Models of Geographical Systems*; Springer: Berlin/Heidelberg, Germany, 2012; pp. 591–610. [[CrossRef](#)]
22. Beaudoin, A.; Isaac, A.G. Direct and indirect transmission of avian influenza: Results from a calibrated agent-based model. *J. Econ. Interact. Coord.* **2023**, *18*, 191–212. [[CrossRef](#)]
23. Gopalappa, C.; Farnham, P.G.; Chen, Y.H.; Sansom, S.L. Progression and Transmission of HIV/AIDS (PATH 2.0): A New, Agent-Based Model to Estimate HIV Transmissions in the United States. *Med. Decis. Mak.* **2017**, *37*, 224–233. [[CrossRef](#)] [[PubMed](#)]
24. Tabasi, M.; Alesheikh, A.A.; Kalantari, M.; Mollalo, A.; Hatamiafkoueih, J. Spatio-Temporal Modeling of COVID-19 Spread in Relation to Urban Land Uses: An Agent-Based Approach. *Sustainability* **2023**, *15*, 13827. [[CrossRef](#)]
25. Wang, L.; Li, X. Spatial epidemiology of networked metapopulation: An overview. *Chin. Sci. Bull.* **2014**, *59*, 3511–3522. [[CrossRef](#)]
26. Humphries, R.; Spillane, M.; Mulchrone, K.; Wiecek, S.; O’Riordain, M.; Hövel, P. A metapopulation network model for the spreading of SARS-CoV-2: Case study for Ireland. *Infect. Dis. Model.* **2021**, *6*, 420–437. [[CrossRef](#)]
27. Calvetti, D.; Hoover, A.P.; Rose, J.; Somersalo, E. Metapopulation Network Models for Understanding, Predicting, and Managing the Coronavirus Disease COVID-19. *Front. Phys.* **2020**, *8*, 261. [[CrossRef](#)]
28. Kasereka, S.K.; Zohinga, G.N.; Kiketa, V.M.; Ngoie, R.B.M.; Mputu, E.K.; Kasoro, N.M.; Kyandoghere, K. Equation-Based Modeling vs. Agent-Based Modeling with Applications to the Spread of COVID-19 Outbreak. *Mathematics* **2023**, *11*, 253. [[CrossRef](#)]
29. Cuevas, E. An agent-based model to evaluate the COVID-19 transmission risks in facilities. *Comput. Biol. Med.* **2020**, *121*, 103827. [[CrossRef](#)]
30. Rodríguez, A.; Cuevas, E.; Zaldivar, D.; Morales-Castañeda, B.; Sarkar, R.; Houssein, E.H. An agent-based transmission model of COVID-19 for re-opening policy design. *Comput. Biol. Med.* **2022**, *148*, 105847. [[CrossRef](#)]
31. Borjigin, S.G.; He, Q.; Niemeier, D.A. COVID-19 transmission in U.S. transit buses: A scenario-based approach with agent-based simulation modeling (ABSM). *Commun. Transp. Res.* **2023**, *3*, 100090. [[CrossRef](#)]
32. Gunaratne, C.; Reyes, R.; Hemberg, E.; O’Reilly, U.M. Evaluating efficacy of indoor non-pharmaceutical interventions against COVID-19 outbreaks with a coupled spatial-SIR agent-based simulation framework. *Sci. Rep.* **2022**, *12*, 6202. [[CrossRef](#)]
33. Cui, Z.; Cai, M.; Zhu, Z.; Chen, G.; Xiao, Y. Impact of Indoor Mobility Behavior on the Respiratory Infectious Diseases Transmission Trends. *IEEE Trans. Comput. Soc. Syst.* **2024**, 1–14. [[CrossRef](#)]
34. Azuma, K.; Yanagi, U.; Kagi, N.; Kim, H.; Ogata, M.; Hayashi, M. Environmental factors involved in SARS-CoV-2 transmission: Effect and role of indoor environmental quality in the strategy for COVID-19 infection control. *Environ. Health Prev. Med.* **2020**, *25*, 66. [[CrossRef](#)]
35. Karimian, H.; Fan, Q.; Li, Q.; Chen, Y.; Shi, J. Spatiotemporal transmission of infectious particles in environment: A case study of COVID-19. *Chemosphere* **2023**, *335*, 139065. [[CrossRef](#)]
36. Reveil, M.; Chen, Y.H. Predicting and preventing COVID-19 outbreaks in indoor environments: an agent-based modeling study. *Sci. Rep.* **2022**, *12*, 16076. [[CrossRef](#)]
37. Navaratnam, S.; Nguyen, K.; Selvaranjan, K.; Zhang, G.; Mendis, P.; Aye, L. Designing Post COVID-19 Buildings: Approaches for Achieving Healthy Buildings. *Buildings* **2022**, *12*, 74. [[CrossRef](#)]
38. Amran, M.; Makul, N.; Fediuk, R.; Borovkov, A.; Ali, M.; Zeyad, A.M. A Review on Building Design as a Biomedical System for Preventing COVID-19 Pandemic. *Buildings* **2022**, *12*, 582. [[CrossRef](#)]
39. Borgonovo, E.; Pangallo, M.; Rivkin, J.; Rizzo, L.; Siggelkow, N. Sensitivity analysis of agent-based models: A new protocol. *Comput. Math. Organ. Theory* **2022**, *28*, 52–94. [[CrossRef](#)]
40. Italian Civil Protection Department. COVID-19 Italia, Monitoraggio Situ-Azione. Available online: <https://github.com/pcm-dpc/COVID-19> (accessed on 30 April 2023).
41. Italian National Institute of Statistics. Italian National Institute of Statistics. Available online: <https://www.istat.it/en/> (accessed on 30 April 2023).
42. Grimm, V.; Berger, U.; Bastiansen, F.; Eliassen, S.; Ginot, V.; Giske, J.; Goss-Custard, J.; Grand, T.; Heinz, S.K.; Huse, G.; et al. A standard protocol for describing individual-based and agent-based models. *Ecol. Model.* **2006**, *198*, 115–126. [[CrossRef](#)]
43. Grimm, V.; Berger, U.; DeAngelis, D.L.; Polhill, J.G.; Giske, J.; Railsback, S.F. The ODD protocol: A review and first update. *Ecol. Model.* **2010**, *221*, 2760–2768. [[CrossRef](#)]
44. Grimm, V.; Railsback, S.; Vincenot, C.; Berger, U.; Gallagher, C.; Deangelis, D.; Edmonds, B.; Ge, J.; Giske, J.; Groeneveld, J.; et al. The ODD Protocol for Describing Agent-Based and Other Simulation Models: A Second Update to Improve Clarity, Replication, and Structural Realism. *J. Artif. Soc. Soc. Simul.* **2020**, *23*, 7. [[CrossRef](#)]
45. Cattaneo, A.; Vitali, A.; Mazzoleni, M.; Previdi, F. An agent-based model to assess large-scale COVID-19 vaccination campaigns for the Italian territory: The case study of Lombardy region. *Comput. Methods Programs Biomed.* **2022**, *224*, 107029. [[CrossRef](#)]
46. Lhous, M.; Zakary, O.; Rachik, M.; Magri, E.M.; Tridane, A. Optimal Containment Control Strategy of the Second Phase of the COVID-19 Lockdown in Morocco. *Appl. Sci.* **2020**, *10*, 7559. [[CrossRef](#)]
47. Mahdzadeh Gharakhanlou, N.; Mesgari, M.S.; Hooshangi, N. Developing an agent-based model for simulating the dynamic spread of Plasmodium vivax malaria: A case study of Sarbaz, Iran. *Ecol. Inform.* **2019**, *54*, 101006. [[CrossRef](#)]
48. Karumanagoundar, K.; Raju, M.; Ponnaiah, M.; Kaur, P.; Viswanathan, V.; Rubeshkumar, P.; Sakthivel, M.; Shanmugiah, P.; Ganeshkumar, P.; Muthusamy, S.K.; et al. Secondary attack rate of COVID-19 among contacts and risk factors, Tamil Nadu, March–May 2020: A retrospective cohort study. *BMJ Open* **2021**, *11*, e051491. [[CrossRef](#)]

49. Tian, T.; Huo, X. Secondary attack rates of COVID-19 in diverse contact settings, a meta-analysis. *J. Infect. Dev. Ctries* **2020**, *14*, 1361–1367. [[CrossRef](#)]
50. Okhue, A.V. Estimation of the probability of reinfection with COVID-19 by the susceptible-exposed-infectious-removed-undetectable-susceptible model. *JMIR Public Health Surveill.* **2020**, *6*, e19097. [[CrossRef](#)]
51. Knobel, P.; Serra, C.; Grau, S.; Ibañez, R.; Diaz, P.; Ferrández, O.; Villar, R.; Lopez, A.F.; Pujolar, N.; Horcajada, J.P.; et al. Coronavirus disease 2019 (COVID-19) mRNA vaccine effectiveness in asymptomatic healthcare workers. *Infect. Control Hosp. Epidemiol.* **2021**, *42*, 1517–1519. [[CrossRef](#)]
52. Mahdizadeh Gharakhanlou, N.; Hooshangi, N. Spatio-temporal simulation of the novel coronavirus (COVID-19) outbreak using the agent-based modeling approach (case study: Urmia, Iran). *Inform. Med. Unlocked* **2020**, *20*, 100403. [[CrossRef](#)]
53. Kerr, C.C.; Stuart, R.M.; Mistry, D.; Abeyseriya, R.G.; Rosenfeld, K.; Hart, G.R.; Núñez, R.C.; Cohen, J.A.; Selvaraj, P.; Hagedorn, B.; et al. Covasim: An agent-based model of COVID-19 dynamics and interventions. *PLoS Comput. Biol.* **2021**, *17*, e1009149. [[CrossRef](#)]
54. Wang, N.N.; Wang, Y.J.; Qiu, S.H.; Di, Z.R. Epidemic spreading with migration in networked metapopulation. *Commun. Nonlinear Sci. Numer. Simul.* **2022**, *109*, 106260. [[CrossRef](#)]
55. Gong, Y.; Small, M. Epidemic spreading on metapopulation networks including migration and demographics. *Chaos* **2018**, *28*, 083102. [[CrossRef](#)]
56. Azak, E.; Karadenizli, A.; Uzuner, H.; Karakaya, N.; Canturk, N.Z.; Hulagu, S. Comparison of an inactivated COVID-19 vaccine-induced antibody response with concurrent natural COVID-19 infection. *Int. J. Infect. Dis.* **2021**, *113*, 58–64. [[CrossRef](#)]
57. Tiyo, B.T.; Schmitz, G.J.H.; Ortega, M.M.; da Silva, L.T.; de Almeida, A.; Oshiro, T.M.; Duarte, A.J.d.S. What Happens to the Immune System after Vaccination or Recovery from COVID-19? *Life* **2021**, *11*, 1152. [[CrossRef](#)]
58. Sheikhi, F.; Yousefian, N.; Tehranipoor, P.; Kowsari, Z. Estimation of the basic reproduction number of Alpha and Delta variants of COVID-19 pandemic in Iran. *PLoS ONE* **2022**, *17*, e0265489. [[CrossRef](#)]
59. Nishiura, H. Correcting the actual reproduction number: A simple method to estimate R_0 from early epidemic growth data. *Int. J. Environ. Res. Public Health* **2010**, *7*, 291–302. [[CrossRef](#)]
60. Locatelli, I.; Trächsel, B.; Rousson, V. Estimating the basic reproduction number for COVID-19 in Western Europe. *PLoS ONE* **2021**, *16*, e0248731. [[CrossRef](#)]

Disclaimer/Publisher’s Note: The statements, opinions and data contained in all publications are solely those of the individual author(s) and contributor(s) and not of MDPI and/or the editor(s). MDPI and/or the editor(s) disclaim responsibility for any injury to people or property resulting from any ideas, methods, instructions or products referred to in the content.